Investigation of P3HT:WO_3 hybrid electrochromic thin films prepared by solution blending doping

Beyza Yedikardeş [a*], Mustafa Altun [b], Esra Zayim [c]

[a] Department of Nano Science & Nano Engineering, Istanbul Technical University, Istanbul, Turkey

[b] Department of Electronics and Communication Engineering, Istanbul Technical University, Istanbul, Turkey

[c] Department of Physics Engineering, Istanbul Technical University, Istanbul, Turkey

*Corresponding author: yedikardes@itu.edu.tr

Abstract

Although poly(3-hexylthiophene) (P3HT) is a promising p-type conjugating polymer to optimize optical and electrical properties, it is known to be chemically unstable. To overcome this unstability, WO_3 incorporated P3HT hybrid thin films has been synthesized by very simple solution blending doping method. Different amounts of WO_3 were added into the P3HT solution and the incorporation of WO_3 particles was confirmed by scanning electron microscopy, atomic force microscopy, and photoluminescence spectroscopy. The electrochemical reactions in 1 M lithium perchlorate ($LiClO_4$)/propylene carbonate (PC) were studied by cyclic voltammetry and by electrochemical impedance spectroscopy. With the increase amount of WO_3 in P3HT, the electrochromic efficiency increases first and then decreases. The optimum concentration was found as 30 wt% of WO_3. The efficient interaction and well distribution between WO_3 and P3HT improves the capacitive properties and electrochromic performance resulting a 110% increase in coloration efficiency (from 220 cm^2/C to 464 cm^2/C). Moreover, WO_3 doped hybrid films shows long-term cyclability than undoped P3HT films. Structural and electrochemical investigations

suggest that the optimum amount of WO_3 doping is an alternative way to obtain high performance and environmentally stable electrochromic devices.

Keywords

P3HT, WO_3, electrochromic, organic - inorganic hybrid thin films

1. Introduction

Electrochromic materials are materials, which can change their colors reversibly under applied bias. A typical electrochromic device composes of an electrochromic layer coated on transparent conductive oxides (FTO, ITO, etc.) referred as working electrode, ion conductive electrolyte and an ion storage layer referred as counter electrode. The applied voltage determines whether ions are being inserted or extracted which means oxidation or reduction, respectively. Most studies within the field of electrochromic has been centered on transition metal oxides. Transition metal oxides as active layers, however, generally needed sophisticated high temperature vacuum evaporation processes. Electrochromic devices incorporating transition metal oxides usually feature low coloration efficiencies and slow response times that inevitably limit their usage area and industrial applications.

In last decades, organic conjugated polymers such as aniline, pyrrole, thiophene, etc. have drawn great attention on field effect transistors, solar cells and chromogenic electronics, in particularly [1], [2]. Due to the fact that their tunable band gap energies, mobile and delocalize π electrons, they can interact with light and store electrical charges so that they show superior electronic and optical properties in comparison with their inorganic counterparts. Furthermore, thanks to their tunable $\pi \rightarrow \pi^*$ transitions, light interaction and charge carrier transport can be controlled [3], [4]. Compared to other conjugated polymers, polythiophenes become prominent due to their advantages such as being more stable, environmentally friendly, fast coloring

response and having more pronounced π→ π* stackings thanks to their regioregular structure. Conjugated electrochromic polymers show at least one color and one bleach state. However, depending on the position of alkyl groups, repeating units and chain orientation, they could give different colors in the redox state.

P3HT is commonly used as a hole transport layer for organic devices such as photovoltaics and field effect transistors. P3HT, with a band gap of ≈ 2eV, covers the visual spectrum of photonic transitions. However, despite its unique electronic and optical properties, there are few studies on its application to electrochromic devices and coloring mechanism is still not being fully understood.

However, the conjugated polymers are often unstable under atmospheric conditions and oxidation of the side chains and thiophene units in the backbone leading to degradation of the polymer [5], [6]. It was reported that the P3HT films show higher optical contrast under high oxidation potentials but shorter lifetimes. It was thought that this shorter life-times can be attributed to the degradation of P3HT forming sulfone and sulfide species [7]. Therefore, the band gaps of the conjugated polymers can be altered by proper incorporation of the dopant molecules to be able to overcome the short lifetimes and instability of the organic active materials used in EC devices [8].

Hybrid materials are synergistic materials that combine the color diversity of organics and stability of inorganic materials resulting better reversibility, higher optical contrast and faster switching response. Kim and co-workers [9] prepared surfactant assisted graphene oxide (GO-ODA) - P3HT complex to improve long-term cyclability of P3HT. Although there is almost no difference between response times, (GO-ODA)-P3HT complex showed higher ΔT% than pure P3HT (22.4% and 17.9%, respectively). Also, the GO−ODA protective layer described here

could effectively enhance the long-term stability of general polymeric EC materials with electrostatic interactions, π-π stacking and s-π interactions.

Amongst the other inorganic transition metal oxides, WO_3 is the most prominent n-type semiconductor with wide band gap (E_g= 2.5 – 3.2 eV) and high electron affinity which provide many distinct properties [10], [11] such as electrochromic [12], photochromic [13] , thermochromic [14], [15], energy storage [16] and heat shielding applications [17], [18].

We have recently reported that [19] excellent electrical charge transfer between P3HT and WO_3 by dispersing WO_3 powders in P3HT/1,2-dichlorobenzene solution. This very simple produced hybrid formulation enhanced hole mobility of P3HT and improved switching performance of field effect transistor. From this point of view, it is highly interesting to study the electrochromic behavior of P3HT:WO_3 hybrid thin films. It is predicted that energy levels and charge carrier density can be altered by incorporating of WO_3 molecules due to the interactions with donor groups of P3HT.

In the present work, very simple solution blending technique has been used to produce electrochromic hybrid thin films. The blends have been prepared with different WO_3 concentrations. It was found that the not only highest optical contrast and coloration efficiency but also the longer cyclability are obtained for 30% in wt. of WO_3 incorporation in P3HT:WO_3 blends. This promising hybrid formulation is expected to be successfully used in third generation electronics, photonics, for energy saving smart windows and flexible sensor applications.

2. Experimental

The indium−tin oxide (ITO) was magnetron sputtered on soda lime silicate glass substrates. ITO glass substrates (≈17 Ω/sq) were sonicated in ethanol and deionized (DI) water for 10 min. Then, the ITO glass substrates were dried with a nitrogen gun. For the working electrode, various

concentrations of WO_3 (0 wt.% , 10 wt.%, 30 wt.%, 50 wt.%) were dispersed in P3HT/1,2-dichlorbenzene solution and spin coated on ITO glasses. The detailed solution preparation and coating procedures were originally reported in our previous study [19]. All electrochemical measurements were performed in atmospheric conditions in a three-electrode cell containing 1 M $LiClO_4$/PC electrolyte. The P3HT/ITO or P3HT:WO_3/ITO thin films, silver/silver chloride (Ag/AgCl) wire and platinum (Pt) wire were used as working electrode, reference electrode and counter electrodes, respectively. Electrochromic thin films with an active area of 1 x 1 cm^2 were characterized by means of cyclic voltammetry (CV) and chronoamperometry (CA) analysis in CHI 6005D model CH Instrument. UV-vis spectra were recorded in situ during potentiostatic measurements. The surface morphology of both pure and WO_3 doped P3HT thin films was characterized by atomic force microscopy (AFM, Veeco Dimension 3100) and field emission gun scanning electron microscopy (SEM, Hitachi SU 8220-FEGSEM, operated at 1.5 kV) electron dispersive x-ray spectroscopy (EDX) connected to FEGSEM with Oxford software.

3. Results and discussion

First, elemental analysis and surface imaging was performed to confirm the presence of tungsten in the prepared WO_3 doped hybrid films. Elemental composition in weight percentages and surface morphology images are given in Table 1 and Figure 1, respectively. As can be seen in Figure 1, the surface of undoped P3HT film has ordered crystalline domains under 60.000x magnification. However, the morphology of the film changes with WO_3 doping. It is observed that the WO_3 particles are homogeneously dispersed on the surface of PW10 (≈28 – 35 nm) and PW30 (≈40 - 50 nm) hybrid films whereas the particles grow and agglomerate in PW50 hybrid film. The average surface roughness (R_a) was determined from AFM analysis and was found as 2.4 nm, 3.7 nm, 8.2 nm, 55.3 nm for undoped P3HT, PW10, PW30 and PW50,

respectively. The AFM images given in Figure 1 also support the FEGSEM images. Undoped P3HT has regular branched and interconnected domains. However, it is seen that when 50% in wt. WO_3 is added into the polymer, large-sized WO_3 particles with a diameter of 150-450 nm agglomerate on the surface so that the average surface roughness significantly increases.

Table 1. Sample codes and elemental composition in weight percentages obtained from energy dispersive spectroscopy of prepared thin films.

Doping concentration	Sample code	C%	O%	Si%	S%	W%	In%	Sn%
0% wt. WO_3	P3HT	21.73	16.93	17.36	4.51	-	37.11	2.36
10% wt. WO_3	PW10	19.83	17.03	18.03	4.22	0.98	37.43	2.48
30% wt. WO_3	PW30	19.54	18.53	18.24	4.38	1.34	35.71	2.26
50% wt. WO_3	PW50	16.40	22.14	15.73	5.13	3.21	34.99	2.40

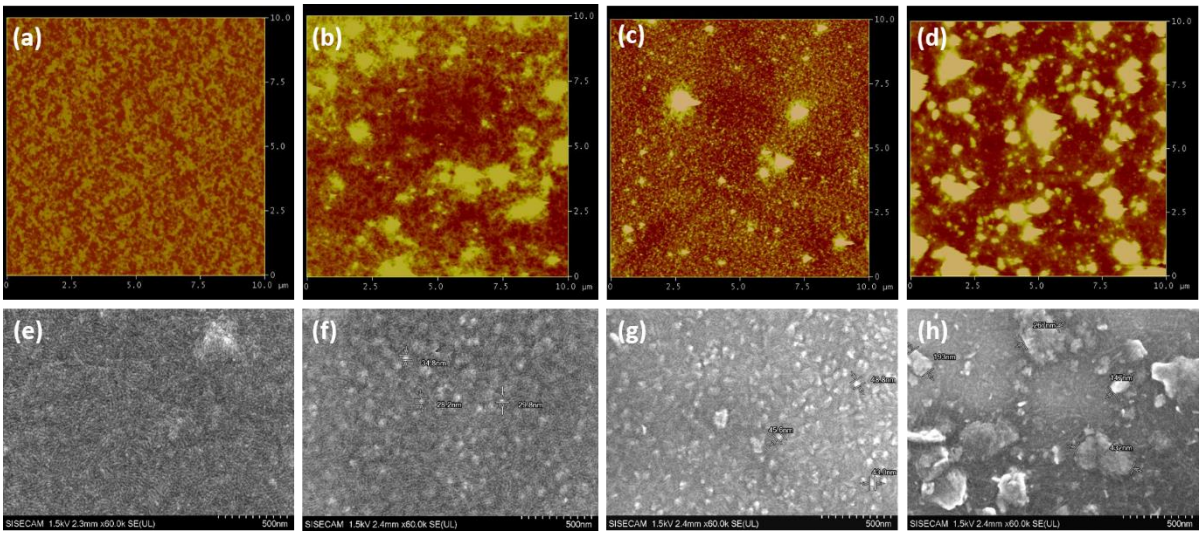

Figure 1. Field emission scanning electron micrographs of **(a)** P3HT, **(b)** PW10, **(c)** PW30, **(d)** PW50 and two dimensional AFM images of **(e)** P3HT, **(f)** PW10, **(g)** PW30, **(h)** PW50.

To investigate the electrochemical behavior of P3HT films, the CV plot recorded at the different scan rates from 50 to 1000 mV s^{-1} in 1 M $LiClO_4$/PC electrolyte and shown in Figure 2a. The CV curve of the P3HT widens up to 1000 mV s^{-1} and maintain its characteristics. This shows that a typical electrochemical capacitive behavior with the rapid ion diffusion. Figure 2b shows

the oxidation (I_{p1}) and reduction (I_{p2}) peak currents depending on the scanning rate. The good linear relationship between the square root of the scan rate and peak current, which means redox behavior is controlled by ions from the electrolyte solution through the electrode surface.

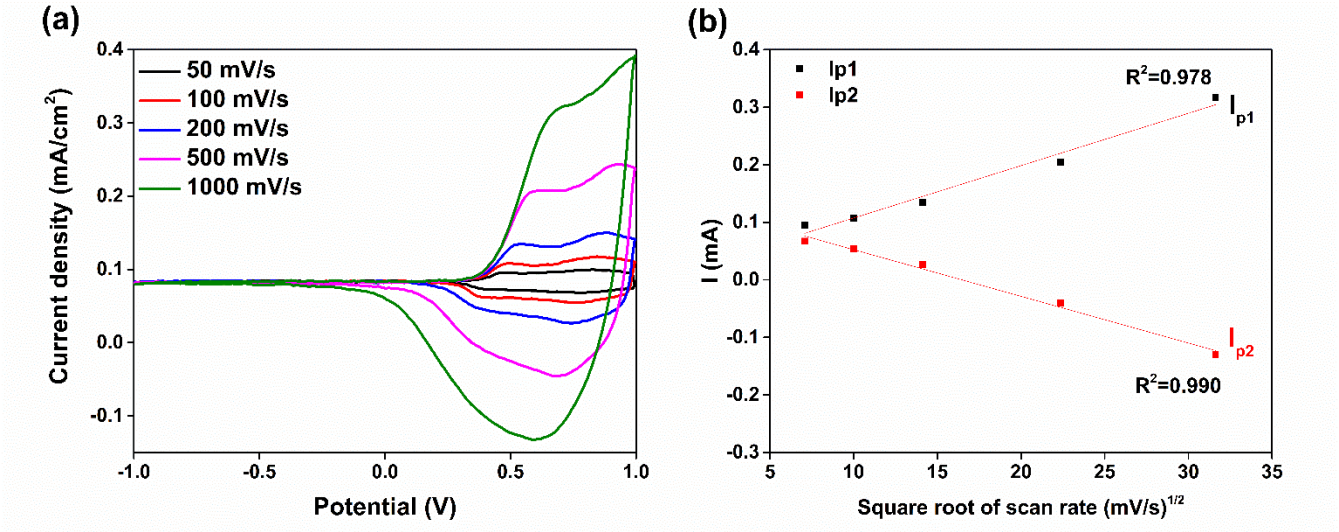

Figure 2. (a) CV plot of P3HT at different scan rates and **(b)** peak current – scan rate square root graph of P3HT.

CV measurements were recorded for each hybrid film to investigate the effect of WO_3 incorporation on redox behavior. The CV curves of both doped and undoped P3HT films under 100 mV s^{-1} scanning of ±1V potential range are shown in Figure 2. It is seen that PW30 shows the lowest oxidation potential ($E^{ox.}_{onset}$=0.25 eV). To be able to discuss the reason of this reduction in oxidation potential, HOMO energy levels of the material can be calculated by using the formula below [20].

$$E_{HOMO} = -(E_{ox.\ onset\ vs.\ Ag/AgCl} + 4.35)\ eV \quad \text{(Eq. 1)}$$

Considering this formula, HOMO levels of electrochromic films were determined as -4.73 eV, -4.69 eV, -4.60 eV and -4.66 eV for P3HT, PW10, PW30 and PW50, respectively. As can be clearly seen, PW30 has a higher HOMO energy level than the other electrochromic films. Strong

donor-acceptor interactions can increase the HOMO energy levels, leading to a decrease in onset oxidation potentials[21], [22]. Therefore, it is thought that efficient WO3 doping may change the electron density of donor groups in P3HT chain since it probably interacts with the thiophene groups by electrostatic interactions, leading to a decrease in oxidation potential. In similar studies [23], [24], significant broadening of CV curve and reduction in oxidation peaks refer to more efficient interaction between host material and dopant molecule, resulting a better charge transfer. This means that it is easier to excite electrons under an applied potential [25]. Besides, the oxidation potential corresponding to the onset potential depends on the interaction between electrodes and electrolyte interface. The areal capacitance (Ca) is calculated with the formula below [26].

$$C_a = \frac{1}{2A\vartheta(\Delta V)} \int idV \qquad \text{(Eq. 2)}$$

Where A is electrode area, ϑ is scan rate, ΔV is applied potential range and integrated i is total charge calculated from the area under the CV curve. PW30 showed the areal capacitance of 1.135 mF/cm^2 whereas P3HT showed the areal capacitance of 0.635 mF/cm^2. These results are parallel to the charge transfer resistance of P3HT and PW30 films measured by impedance spectroscopy given in Figure 8. . There is no further coloring observed between the potential range of 0V and -1V.

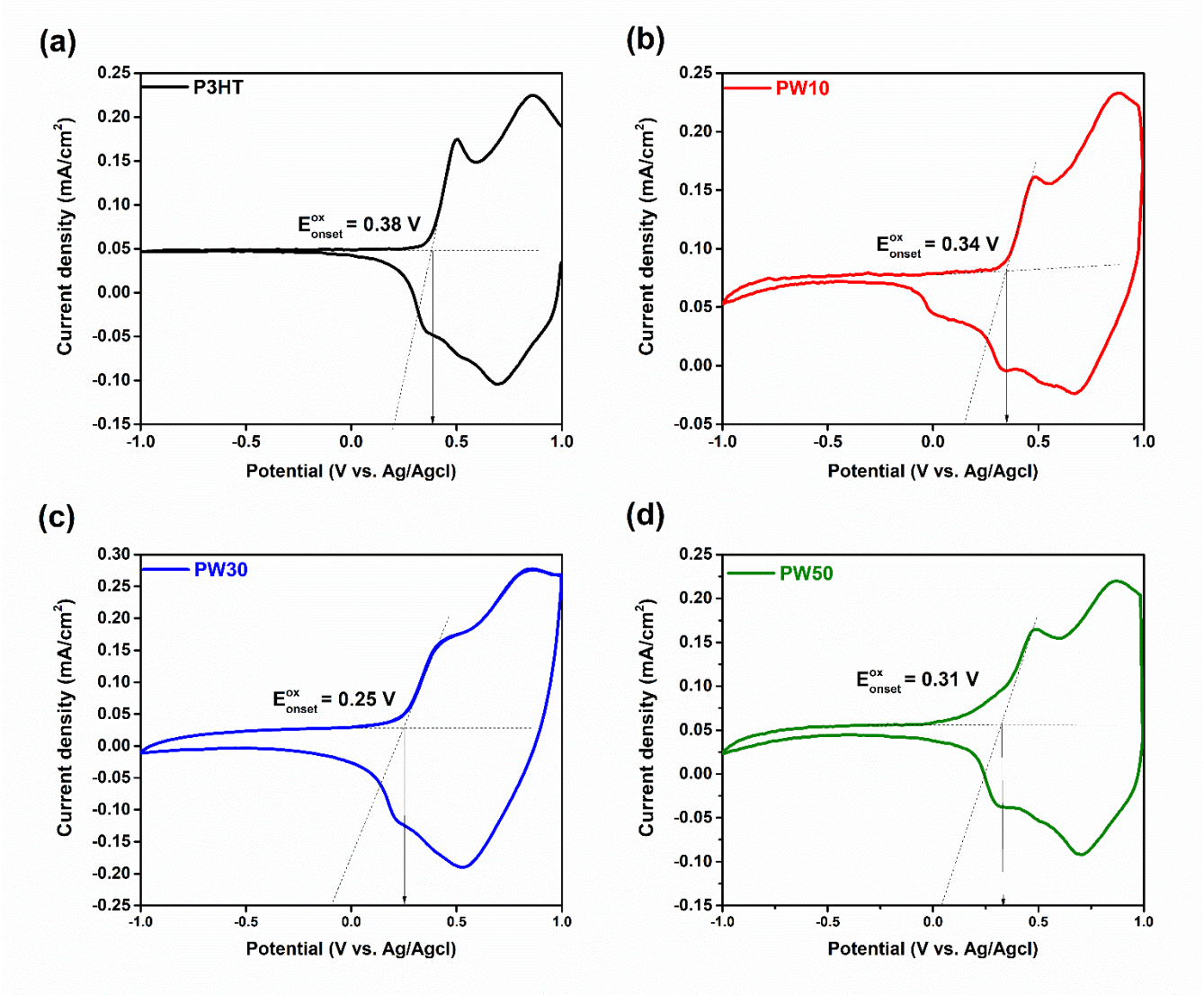

Figure 3. Cyclic voltammograms at 100 mV/s of **(a)** P3HT, **(b)** PW10, **(c)** PW30 and **(d)** PW50 in 1 M $LiClO_4$/PC electrolyte solution.

After electrochemical characterizations, the reversibility of the electrochromic films was tested by chronoamperometry (CA) cycling and UV-vis spectra at 550 nm was recorded in situ in 0V-1V potential range within 8 s time interval. Figure 4 shows the response of color change occurred by charging/discharging of working electrode. When a positive bias (+1V) is applied to the thin films coated on ITO glass, both doped and undoped P3HT thin films oxidize and change color from purple to transparent following the reaction below (Eq. 3). Upon oxidation, doped and

undoped P3HT thin films are doped with ClO_4^- counter anions by forming delocalize π-electron band structures. Under even in 0V, bipolaronic state of the polymer reduces by anion extraction (or cation insertion from electrolyte solution) and turns back to the neutral state. Both doped and undoped P3HT films show one bleach and one colored state.

$$P3HT^0 + ClO_4^- \underset{\text{polaronic}}{\longleftrightarrow} P3HT^+ClO_4^- \underset{\text{bipolaronic}}{\longleftrightarrow} P3HT^{+2}2ClO_4^- \quad \text{(Eq. 3)}$$

Considering the Fig. 4, the maximum transmittance difference ($\Delta T\% = T_{bleach} - T_{color}$) and the maximum optical density ($OD = \log(T_{bleach}/T_{color})$ was found as 36% and 0.26 for PW30 at 550 nm, respectively. The coloration efficiency was calculated using the Equation 4, where ΔOD and Q_{in} indicate the change of optical density and injected charges for 1 cm^2 electrode area, respectively. The coloration efficiency (η) was determined to be 464 cm^2/C for PW30. This value is almost twice that of the undoped P3HT film (220 cm2/C). The optical properties of electrochromic films are reported in Table 2. As can be seen in Table 2, the injected charge densities of 1.10 $mC.cm^{-2}$ and 0.59 $mC.cm^{-2}$ for P3HT and PW30 at +1V. Since the PW30 films show high transmittance modulation even in small charge injections, high coloration efficiency is obtained. This means a lower oxidation potential would suffice to induce bleaching, which makes the charges to be excited easier. Furthermore, coloration efficiency can be affected by both doping efficiency and morphology. Several studies reported that the larger coloration efficiency can be obtained by increasing conductive network by producing polymer composites [27], [28], [29]. Besides, since the active surface area (average surface roughness) of PW30 calculated from AFM is higher than P3HT, this may allow efficient interaction of ClO_4^- ions at the electrode-electrolyte interface, thereby providing the higher optical modulation. In both cases, lower interface resistance is provided.

Since there is no significant improvement on electrochemical properties, PW10 and PW50 hybrid thin films were eliminated and were not tested through long cycles. It is also thought that the reason of lower optical contrast for PW50 is due to either the aggregated WO_3 particles given in Figure 1 or disconnection of π-stacking (crystalline aggregates) with excess amount of

WO_3. This may also lead to an increase in trapped charge carriers, decreasing the electrical and optical properties [30].

The long term performance of P3HT and PW30 was measured by observing the transmittance change over time while continuously switching between the colored and bleached states (Figure 5). There is almost no change in transmittance difference of PW30 during 1000 cycle whereas the transmittance difference decreases from 32% to 23% for P3HT. Since the stability and electrochromic performance parameters of PW30 is better than P3HT, further characterizations were performed comparatively for only PW30 and P3HT.

$$\eta = \frac{\Delta OD}{Q_{in}} \qquad \text{(Eq. 4)}$$

Table 2. The optical properties of pure and doped P3HT thin films at 550 nm.

Doping concentration	Sample code	T_{bleach}%	T_{color}%	ΔT%	ΔOD	Q_{in} (mC/cm^2)	Q_{out} (mC/cm^2)	η (cm^2/C)
0% wt. WO_3	P3HT	75.57	43.27	32.3	0.24	1.10	1.02	220
10% wt. WO_3	PW10	75.66	43.76	31.9	0.24	1.01	0.78	233
30% wt. WO_3	PW30	79.70	42.70	37.0	0.26	0.59	0.61	464
50% wt. WO_3	PW50	70.53	43.01	27.5	0.21	0.50	0.53	422

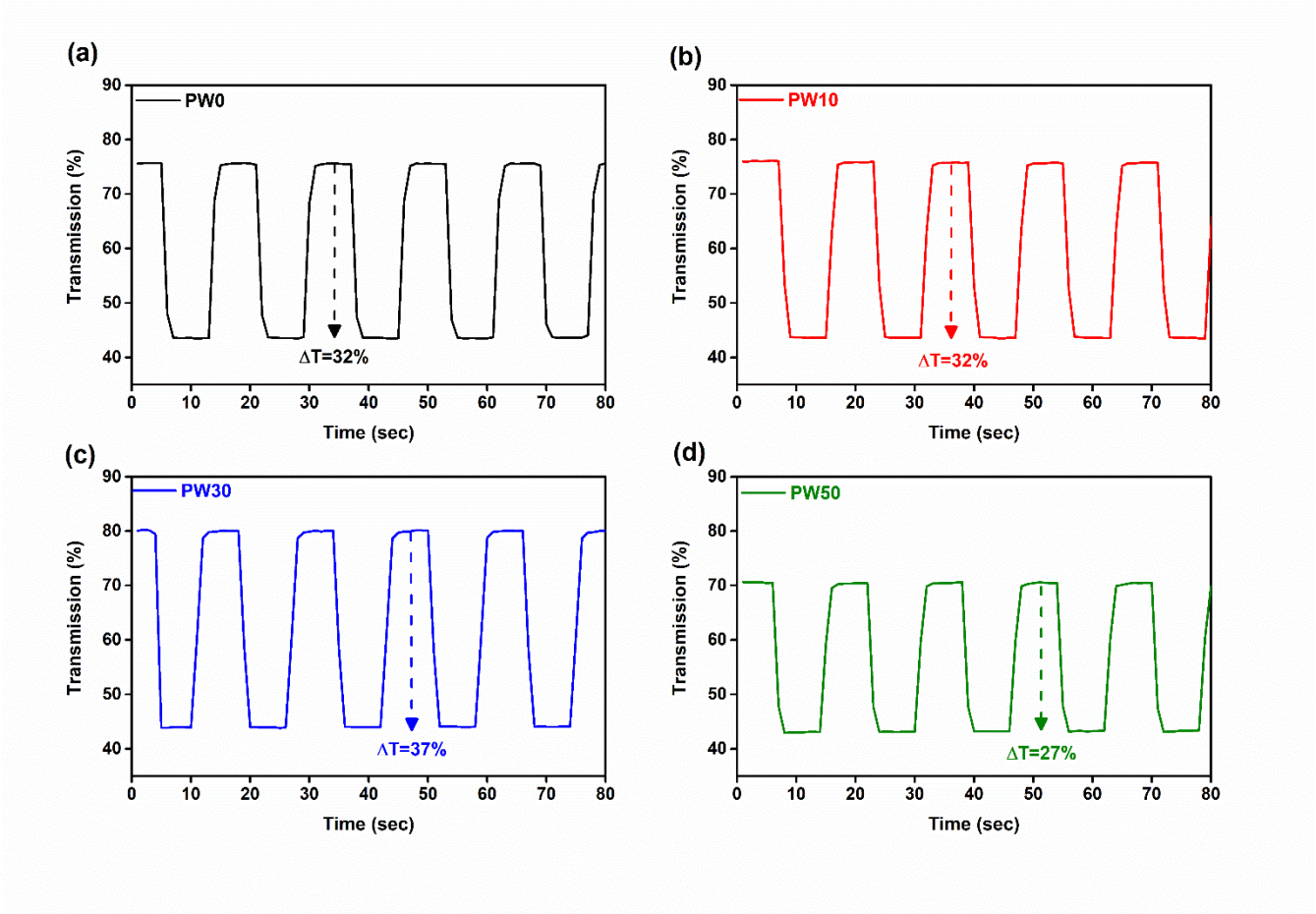

Figure 4. Optical contrast of **(a)** P3HT, **(b)** PW10, **(c)** PW30, and **(d)** PW50 thin films with a residence time of 8 s.

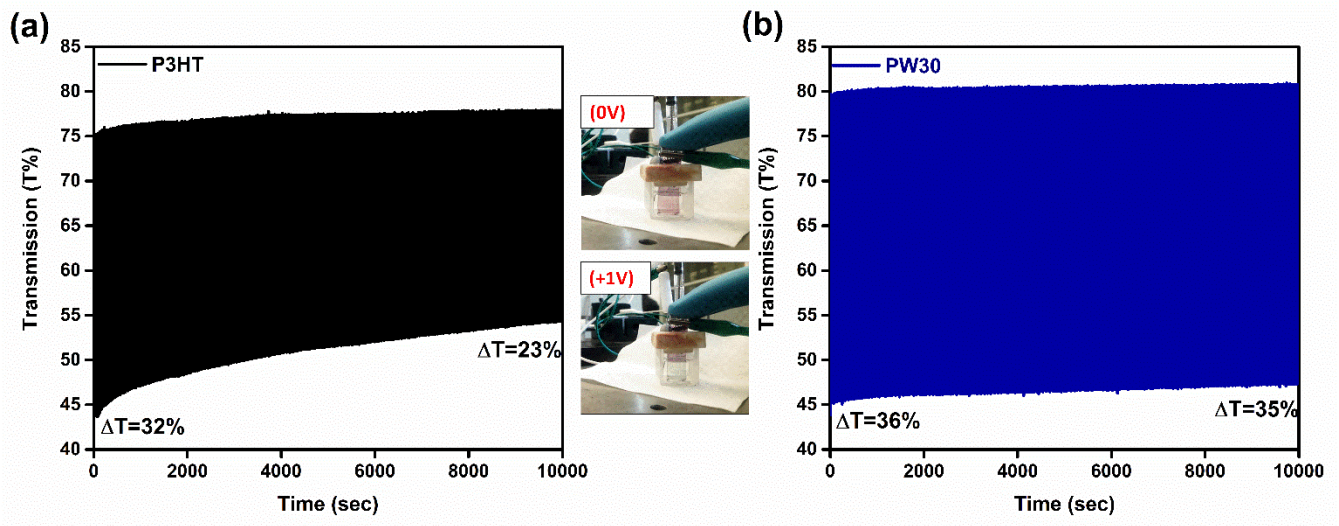

Figure 5. Long-term electrochemical cycling stability measurements of the **(a)** P3HT and **(b)** PW30 thin films with a residence time of 5 s.

The UV visible absorption spectra for P3HT and PW30 are given in Figure 6a. For P3HT film, two distinct peaks at 512 nm and 546 nm and a shoulder at 603 nm are observed, showing the maximum peak at 546 nm. These peaks can be ascribed to π→π* interactions in conjugated P3HT chains. After the doping of 30%wt. WO3 into the P3HT, the absorption peak broadens. Similar to previous studies [31], [32], the broadening of the absorption spectrum with the addition of the dopant molecule to the host material indicates that there is an interaction between two materials. It can be said that the reason of this broadening is due to electrostatic interactions for this study. The vibrational energies of WO_3 molecules may contribute to the absorption band of P3HT. Since the peak intensity depends on the crystalline degree, the shoulder at 603 nm may be indicate higher crystallization order of the P3HT chains in the PW30 hybrid structure. In our previous study [19], it was also confirmed the crystalline reflections of WO_3 particles became visible in PW30 hybrid film by XRD and Raman analysis. PL quenching is one of the powerful measurement methods for determining the charge transfer efficiency in the donor-acceptor

blends. PL spectra of P3HT and PW30 excited at 422 nm is given in Figure 6b. Maximum emission peak and a shoulder is observed at 598 nm and 632 nm, respectively. PL intensity quenches after the incorporation of 30% wt. WO_3, which indicates the charge transfer and the creation/dissociation of the excitons between WO_3 and P3HT [32–37]. In the light of these findings, it is hypothesized that higher exciton dissociation efficiency and favorable donor – acceptor interactions between thiophene units of P3HT and WO_3 particles increases the HOMO energy level of P3HT by reducing the oxidation onset potential. Therefore, PW30 thin film shows a lower onset potential of oxidation than that of pure P3HT resulting an improvement in optical contrast.

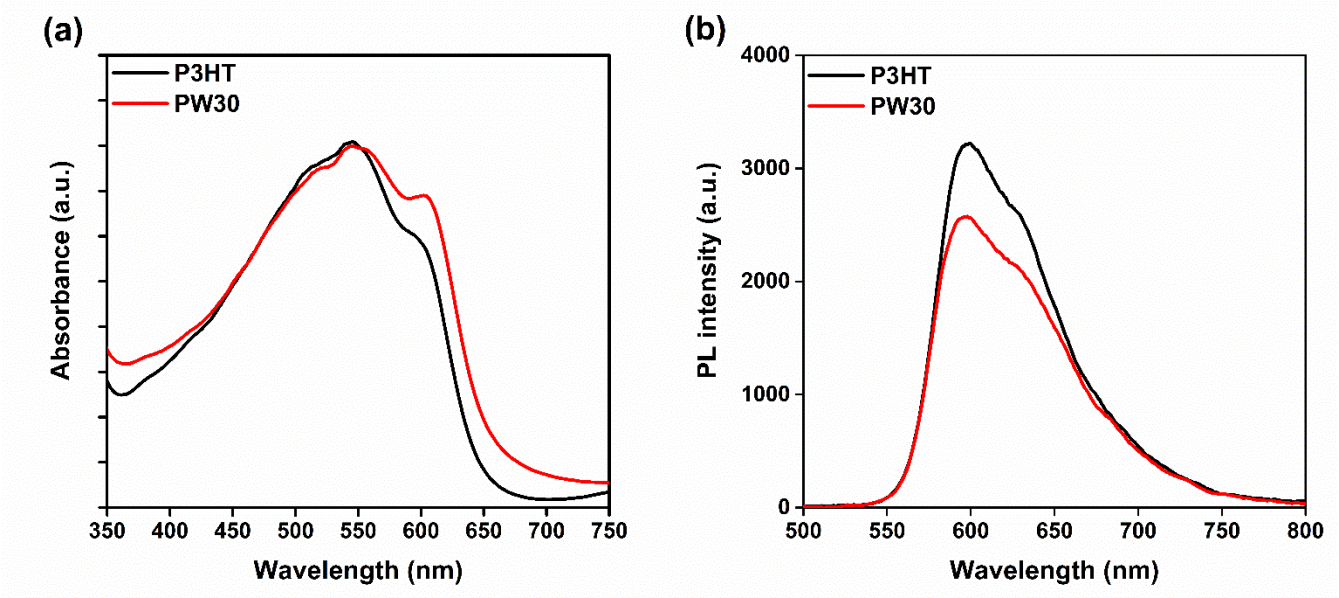

Figure 6. (a) UV-visible absorption spectra and **(b)** PL spectra of P3HT and PW30.

The energy gap between the highest occupied π-electron band (valence band or HOMO) and the lowest unoccupied band (the conduction band or LUMO) determines the intrinsic optical properties of these materials. Hence, the optical band gap was calculated for both P3HT and PW30 films by using Tauc plot with the aid of the equation below;

$$(\alpha h\upsilon)^{\frac{1}{n}} = h\upsilon - E_{gap} \quad \text{(Eq. 5)}$$

where h is the Planck constant, υ is the frequency, E_{gap} is the optical band gap energy and the exponent n indicates the nature of the band transition with direct allowed, indirect allowed, direct forbidden and indirect forbidden transitions which related to the value of 1/2, 2, 3/2, and 3, respectively. The absorption coefficient (α) was calculated by using Beer Lambert law as a function of absorbance and film thickness ($\alpha=2.303A/d_{film}$). Herein, d_{film} is the film thickness and found as ≈80 nm for P3HT and ≈88 nm for WO_3 doped P3HT. The optical band gap is obtained from the extrapolation of the linear part of the plot $(\alpha h\upsilon)^2$ versus hυ. As can be seen in Tauc plot in Figure 7, optical energy gap (E_g) values were found to decrease from 1.95 eV to 1.92 eV with the addition of WO_3 particles attributed the delocalization of charges [38]. Narrower bandgap and suitable energy levels lower the oxidation potential and provide higher onset of absorbance resulting the substantial optical contrast [21].

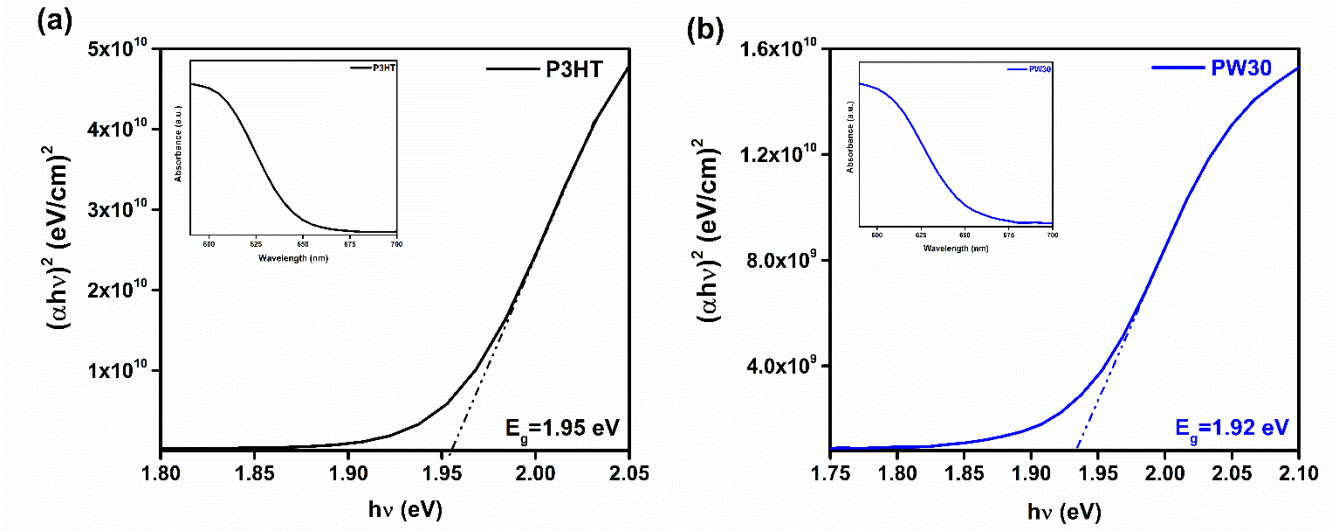

Figure 7. Tauc plots derived from UV-visible absorption spectra of **(a)** P3HT and **(b)** PW30.

Electrochemical impedance spectroscopy (EIS) measurements were also performed in the frequency range of 1 MHz–0.01 Hz to investigate the electron transfer at the electrochromic film

and electrolyte solution interface. As shown in Figure 8, the diameter of the semi-circles in the high frequency region indicates the charge transfer resistance (R_{ct}) of the electrochromic films and decreases from 2.4 Ω to 1.3 Ω with the addition of 30% wt. WO_3 particles. PW30 film has a smaller circle radius due to the efficient donor- acceptor structure between thiophene units and better charge mobility. The switching time during bleaching (coloring) were 1.65 s (1.05 s) for P3HT and 1.04 s (0.95 s). PW30 has lower charge transfer impedance in high frequency region so that the redox and electrochromic reactions are proceeded easily due to the good ionic conductivity, and electrochromic performance of hybrid film was improved compared to undoped P3HT [39].

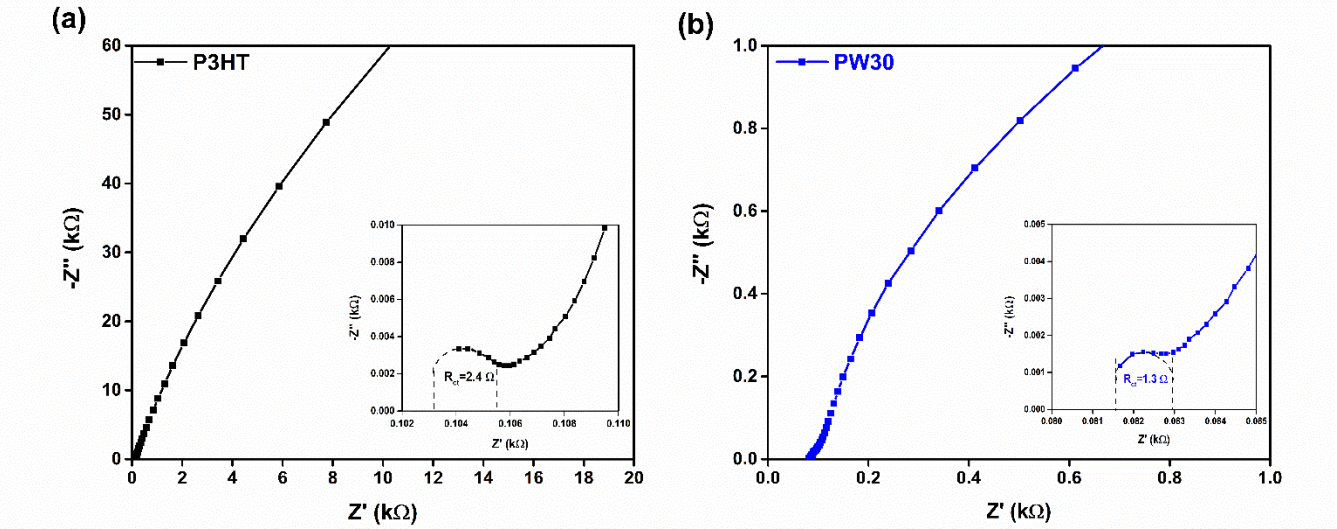

Figure 8. (a) Nyquist plots of **(a)** P3HT and **(b)** PW30 films.

Bode plots indicate the capacitive behaviour of electrochromic films at low-frequency region. Low-frequency capacitance (C_{LF}) were calculated from the slope of Bode plot using the equation below; where f is frequency and Z_{im} is imaginary part of the impedance.

$$C_{LF} = \frac{1}{2\pi f Z_{im}} \qquad \text{(Eq. 6)}$$

C_{LF} values of P3HT and PW30 were changed from $3.6x10^{-5}$ F to $184x10^{-5}$ F. Double layer capacitance (C_{DL}) indicates the accumulation of charges at the electrode-electrolyte interface and it is calculated applying Bode magnitude (|Z|) at 0.16 Hz freqeuncy (log ω = 0). C_{DL} is calculated as 5.7 µF and 105 µF for P3HT and PW30, respectively. EIS studies confirm that PW30 hybrid thin films have improved capacitive behaviour which means better storage.

$$|Z|_{(f=0.16)} = \frac{1}{c_{DL}} \quad \text{(Eq. 7)}$$

4. Conclusion

WO_3 doped P3HT thin films in different doping concentrations were prepared by simple solution blending method. 30% WO_3 in wt. doped P3HT shows efficient interaction resulting an improvement in electrochromic performance. Almost 110% increase in coloration efficiency was achieved in PW30 thin films compared to P3HT and long cycle device stability was significantly improved. EIS measurements show that optimum amount of WO_3 addition in P3HT improves the capacitive properties, which presents a promising candidate for electrical double-layer (EDL) capacitors. Based on these results, it is though that WO_3/P3HT organic-inorganic hybrid thin films can facilitate in development of electrochromic energy storage applications in near future.

Acknowledgement

Thanks to financial supports from Scientific Research Projects realized at Istanbul Technical University (No. 42184).

References

[1] S.B. Mdluli, M.E. Ramoroka, S.T. Yussuf, K.D. Modibane, V.S. John-Denk, E.I. Iwuoha, π-Conjugated Polymers and Their Application in Organic and Hybrid Organic-Silicon Solar Cells, Polymers (Basel). 14 (2022). https://doi.org/10.3390/polym14040716.

[2] Z. Qiu, B.A.G. Hammer, K. Müllen, Conjugated polymers – Problems and promises, Prog. Polym. Sci. (2020). https://doi.org/10.1016/j.progpolymsci.2019.101179.

[3] A.C. Grimsdale, K.L. Chan, R.E. Martin, P.G. Jokisz, A.B. Holmes, Synthesis of light-emitting conjugated polymers for applications in electroluminescent devices, Chem. Rev. (2009). https://doi.org/10.1021/cr000013v.

[4] T.K. Das, S. Prusty, Review on Conducting Polymers and Their Applications, Polym. - Plast. Technol. Eng. (2012). https://doi.org/10.1080/03602559.2012.710697.

[5] K. Wang, Y. Li, Y. Li, Challenges to the Stability of Active Layer Materials in Organic Solar Cells, Macromol. Rapid Commun. (2020). https://doi.org/10.1002/marc.201900437.

[6] M. Manceau, A. Rivaton, J.L. Gardette, S. Guillerez, N. Lemaître, The mechanism of photo- and thermooxidation of poly(3-hexylthiophene) (P3HT) reconsidered, Polym. Degrad. Stab. (2009). https://doi.org/10.1016/j.polymdegradstab.2009.03.005.

[7] T.H. Kim, S. Hyun Song, H.J. Kim, S.H. Oh, S.Y. Han, G. Kim, Y.C. Nah, Effects of oxidation potential and retention time on electrochromic stability of poly (3-hexyl thiophene) films, Appl. Surf. Sci. (2018). https://doi.org/10.1016/j.apsusc.2018.02.141.

[8] X. Fu, C. Jia, Z. Wan, X. Weng, J. Xie, L. Deng, Hybrid electrochromic film based on polyaniline and TiO2 nanorods array, Org. Electron. (2014). https://doi.org/10.1016/j.orgel.2014.07.040.

[9] T.H. Kim, K.I. Choi, H. Kim, S.H. Oh, J. Koo, Y.C. Nah, Long-Term Cyclability of Electrochromic Poly(3-hexyl thiophene) Films Modified by Surfactant-Assisted Graphene Oxide Layers, ACS Appl. Mater. Interfaces. (2017). https://doi.org/10.1021/acsami.7b04184.

[10] F. Wang, C. Di Valentin, G. Pacchioni, Electronic and structural properties of WO3: A systematic hybrid DFT study, J. Phys. Chem. C. (2011). https://doi.org/10.1021/jp201057m.

[11] L.G. Gerling, S. Mahato, C. Voz, R. Alcubilla, J. Puigdollers, Characterization of transition metal oxide/silicon heterojunctions for solar cell applications, Appl. Sci. (2015). https://doi.org/10.3390/app5040695.

[12] V.R. Buch, A.K. Chawla, S.K. Rawal, Review on electrochromic property for WO3 thin films using different deposition techniques, in: Mater. Today Proc., 2016. https://doi.org/10.1016/j.matpr.2016.04.025.

[13] S. Wang, W. Fan, Z. Liu, A. Yu, X. Jiang, Advances on tungsten oxide based photochromic materials: Strategies to improve their photochromic properties, J. Mater. Chem. C. (2018). https://doi.org/10.1039/c7tc04189f.

[14] S. Long, H. Zhou, S. Bao, Y. Xin, X. Cao, P. Jin, Thermochromic multilayer films of WO3/VO2/WO3 sandwich structure with enhanced luminous transmittance and durability, RSC Adv. (2016). https://doi.org/10.1039/c6ra23504b.

[15] I. Top, R. Binions, C. Sol, I. Papakonstantinou, M. Holdynski, S. Gaiaschi, I. Abrahams, Improved thermochromic properties in bilayer films of VO2 with ZnO, SnO2 and WO3 coatings for energy efficient glazing, J. Mater. Chem. C. (2018). https://doi.org/10.1039/c8tc04543g.

[16] W. Han, Q. Shi, R. Hu, Advances in Electrochemical Energy Devices Constructed with Tungsten Oxide-Based Nanomaterials, Nanomaterials. (2021). https://doi.org/10.3390/nano11030692.

[17] C.W. Chang-Jian, E.C. Cho, S.C. Yen, B.C. Ho, K.C. Lee, J.H. Huang, Y.S. Hsiao,

Facile preparation of WO3/PEDOT:PSS composite for inkjet printed electrochromic window and its performance for heat shielding, Dye. Pigment. (2018). https://doi.org/10.1016/j.dyepig.2017.09.026.

[18] C. Yang, J.F. Chen, X. Zeng, D. Cheng, D. Cao, Design of the alkali-metal-doped WO3 as a near-infrared shielding material for smart window, Ind. Eng. Chem. Res. (2014). https://doi.org/10.1021/ie503284x.

[19] B. Yedikardeş, F. Ordokhani, N. Akkan, E. Kurt, N.K. Yavuz, E. Zayim, M. Altun, Enhanced Electrical Properties of P3HT:WO3 Hybrid Thin Film Transistors, J. Electron. Mater. (2021). https://doi.org/10.1007/s11664-021-08764-4.

[20] S. Wang, S. Cai, W. Cai, H. Niu, C. Wang, X. Bai, W. Wang, Y. Hou, Organic-inorganic hybrid electrochromic materials, polysilsesquioxanes containing triarylamine, changing color from colorless to blue, Sci. Rep. (2017). https://doi.org/10.1038/s41598-017-15337-1.

[21] Y. Zhang, L. Kong, Y. Zhang, H. Du, J. Zhao, S. Chen, Y. Xie, Y. Wang, Ultra-low-band gap thienoisoindigo-based ambipolar type neutral green copolymers with ProDOT and thiophene units as NIR electrochromic materials, Org. Electron. (2020). https://doi.org/10.1016/j.orgel.2020.105685.

[22] M.C. Scharber, N.S. Sariciftci, Low Band Gap Conjugated Semiconducting Polymers, Adv. Mater. Technol. (2021). https://doi.org/10.1002/admt.202000857.

[23] W.J. Bae, A.R. Davis, J. Jung, W.H. Jo, K.R. Carter, E.B. Coughlin, One-pot synthesis of hybrid TiO2-polyaniline nanoparticles by self-catalyzed hydroamination and oxidative polymerization from TiO 2-methacrylic acid nanoparticles, Chem. Commun. (2011). https://doi.org/10.1039/c1cc13137k.

[24] A. Baray-Calderón, J. Camacho-Cáceres, F. Hernández-Guzmán, H. Hu, M.E. Nicho, Enhanced performance of poly(3-hexylthiophene)-based electrochromic devices by adding a mesoporous TiO2 layer, Synth. Met. (2023). https://doi.org/10.1016/j.synthmet.2022.117274.

[25] R. Li, H. Xu, Y. Zhang, L. Chang, Y. Ma, Y. Hou, S. Miao, C. Wang, Electrochromic properties of pyrene conductive polymers modified by chemical polymerization, RSC Adv. (2021). https://doi.org/10.1039/d1ra07977h.

[26] S. Park, H. Lee, Y.J. Kim, P.S. Lee, Fully laser-patterned stretchable microsupercapacitors integrated with soft electronic circuit components, NPG Asia Mater. (2018). https://doi.org/10.1038/s41427-018-0080-z.

[27] S. Bhandari, M. Deepa, A.K. Srivastava, C. Lal, R. Kant, Poly(3,4-ethylenedioxythiophene) (PEDOT)-Coated MWCNTs Tethered to Conducting Substrates: Facile Electrochemistry and Enhanced Coloring Efficiency, Macromol. Rapid Commun. (2009). https://doi.org/10.1002/marc.200800722.

[28] S. Bhandari, M. Deepa, A.K. Srivastava, A.G. Joshi, R. Kant, Poly(3,4-ethylenedioxythiophene)-multiwalled carbon nanotube composite films: Structure-directed amplified electrochromic response and improved redox activity, J. Phys. Chem. B. (2009). https://doi.org/10.1021/jp9012976.

[29] S. Xiong, J. Wei, P. Jia, L. Yang, J. Ma, X. Lu, Water-processable polyaniline with covalently bonded single-walled carbon nanotubes: Enhanced electrochromic properties and impedance analysis, ACS Appl. Mater. Interfaces. (2011). https://doi.org/10.1021/am101133q.

[30] I.E. Jacobs, E.W. Aasen, J.L. Oliveira, T.N. Fonseca, J.D. Roehling, J. Li, G. Zhang,

M.P. Augustine, M. Mascal, A.J. Moulé, Comparison of solution-mixed and sequentially processed P3HT:F4TCNQ films: Effect of doping-induced aggregation on film morphology, J. Mater. Chem. C. (2016). https://doi.org/10.1039/c5tc04207k.

[31] S. Dayal, N. Kopidakis, D.C. Olson, D.S. Ginley, G. Rumbles, Direct synthesis of CdSe nanoparticles in poly(3-hexylthiophene), J. Am. Chem. Soc. (2009). https://doi.org/10.1021/ja9067673.

[32] F. Alam, N. Kumar, V. Dutta, Study of surfactant-free lead sulfide nanocrystals-P3HT hybrid polymer solar cells, Org. Electron. (2015). https://doi.org/10.1016/j.orgel.2015.03.032.

[33] G.F. Malgas, C.J. Arendse, S. Mavundla, F.R. Cummings, Interfacial analysis and properties of regioregular poly(3-hexyl thiophene) spin-coated on an indium tin oxide-coated glass substrate, J. Mater. Sci. (2008). https://doi.org/10.1007/s10853-008-2797-5.

[34] Y. Firdaus, E. Vandenplas, Y. Justo, R. Gehlhaar, D. Cheyns, Z. Hens, M. Van Der Auweraer, Enhancement of the photovoltaic performance in P3HT: PbS hybrid solar cells using small size PbS quantum dots, J. Appl. Phys. (2014). https://doi.org/10.1063/1.4894404.

[35] M. Zhong, D. Yang, J. Zhang, J. Shi, X. Wang, C. Li, Improving the performance of CdS/P3HT hybrid inverted solar cells by interfacial modification, Sol. Energy Mater. Sol. Cells. (2012). https://doi.org/10.1016/j.solmat.2011.09.041.

[36] F. Li, Y. Du, Y. Chen, L. Chen, J. Zhao, P. Wang, Direct application of P3HT-DOPO@ZnO nanocomposites in hybrid bulk heterojunction solar cells via grafting P3HT onto ZnO nanoparticles, in: Sol. Energy Mater. Sol. Cells, 2012.

https://doi.org/10.1016/j.solmat.2011.09.002.

[37] L. Wang, Y.S. Liu, X. Jiang, D.H. Qin, Y. Cao, Enhancement of photovoltaic characteristics using a suitable solvent in hybrid polymer/multiarmed CdS nanorods solar cells, J. Phys. Chem. C. (2007). https://doi.org/10.1021/jp0715777.

[38] L. Yesappa, M. Niranjana, S. Ashokkumar, H. Vijeth, S. Raghu, H. Devendrappa, Characterization, Electrical Conductivity and Electrochemical Performance of Polyaniline-LiClO4-CuO Nano Composite for Energy Storage Applications, Polym. Technol. Mater. (2019). https://doi.org/10.1080/03602559.2018.1466175.

[39] Y.E. Firat, A. Peksoz, Efficiency enhancement of electrochromic performance in NiO thin film via Cu doping for energy-saving potential, Electrochim. Acta. (2019). https://doi.org/10.1016/j.electacta.2018.10.166.